Nonradiative annihilation of a positron on bound electrons

B. Najjari,[1] S. F. Zhang,[1] X. Ma,[1] and A. B. Voitkiv[2]
[1]*Institute of Modern Physics, Chinese Academy of Sciences, Lanzhou 730000, China*
[2]*Institute for Theoretical Physics I, Heinrich-Heine-University of Düsseldorf, Universitätsstrasse 1, 40225 Düsseldorf, Germany*

(Received 5 March 2020; accepted 6 April 2020; published 27 April 2020)

We consider nonradiative annihilation of a positron on electrons bound by the field of a heavy nucleus. This process proceeds via the interaction of the annihilating positron-electron pair with another bound electron which is emitted carrying away the energy release. We present a fully relativistic treatment of this process which employs exact Dirac wave functions to describe the motion of the leptons in the nuclear field and regards the interaction between the leptons as a perturbation. We calculate the total cross section for this process for a number of elements ranging from silver to fermium. Our results substantially deviate from those previously reported in the literature, both for the absolute values of the cross section and its dependence on the energy of the incident positron. However, when we combine our results and the principle of detailed balance to get the cross section for the inverse process (so-called negative-continuum dielectronic recombination), a very good agreement is found with the existing results obtained by direct calculations. We also compare nonradiative annihilation with radiative annihilation proceeding with emission of a single photon and show that the cross sections for the former are much smaller.

DOI: 10.1103/PhysRevA.101.042707

I. INTRODUCTION

Positron-electron annihilation represents a fundamental phenomenon of converting matter particles into energy. It can be realized via a few basic mechanisms (processes). The simplest of them is annihilation of a free positron-electron pair, which proceeds with emission of radiation and—due to the energy-momentum constraints—has to involve at least two emitted photons. The total cross section for this process, which was first investigated by Dirac [1], reaches a maximum when the kinetic energy of the relative motion of the pair tends to zero.

More mechanisms for annihilation arise when a positron is incident on an atom. First, the positron can annihilate with outer-shell electrons. The energy release in annihilation given by $\simeq 2m_e c^2 \approx 1$ MeV, where m_e is the mass of the electron (positron) and c the speed of light, is enormous compared to the binding energies of the outer atomic electrons. Therefore, outer atomic electrons in this process can be regarded as (quasi)free and the physics of positron annihilation on them is essentially reduced to that of annihilation of a free positron-electron pair.

Second, with an increase in the electron binding energy, the nucleus of the atom can more effectively participate in the momentum balance of annihilation. As a result, annihilation can also proceed via emission of just a single photon (see Fig. 1) and, at sufficiently large binding energies, this begins to dominate over the two-photon annihilation. This single-photon annihilation mechanism was first considered by Fermi and Uhlenbeck [2]; their studies were followed by other authors [3,4]. In order to be able to annihilate with a tightly bound electron, the incident positron has to penetrate rather close to the atomic nucleus and, hence, initially possess a sufficient kinetic energy. However, with an excessive increase in the positron energy, the time interval, when the positron and electron become close and thus the annihilation can occur, will decrease. As a result, the cross section for this process exhibits a nonmonotonous behavior with the positron kinetic energy, vanishing both at very small and very large values of this energy.

Third, annihilation of an incident positron with a bound electron in the presence of another (neighbor) bound electron can proceed even without emission of radiation. In such a case, the released energy is taken by the neighbor electron (see Fig. 2). The probability of such annihilation, which will be referred to as nonradiative annihilation (NRA), depends on the distance between the electrons. Electrons are most tightly "packed" in inner shells of very heavy atoms and/or ions with their density growing with the increase in the charge Z of the nucleus. Therefore, provided the incident positron has enough energy to come close to the inner electrons, the efficiency of this annihilation mechanism increases when Z grows.

Nonradiative annihilation was first investigated by Brunings [5]. In his calculations, based on a number of approximations, he predicted, for positron annihilation involving two K-shell electrons of lead, a maximum annihilation cross section of $\sim 1 \times 10^{-26}$ cm^2, which is reached at positron kinetic energies between 50 and 300 keV.

Later on, this channel was considered by Massey and Burhop [6], who used plane waves to describe the ejected electron. The authors found, for NRA involving two K-shell electrons of lead atoms, the cross section of 0.1×10^{-26} cm^2 at 100 keV positron kinetic energy. In addition, they also considered NRA, which involves the assisting electron from higher shells, and concluded that the cross section can reach a maximum value between 1 and 1.5×10^{-26} cm^2 at 300 keV positron kinetic energy.

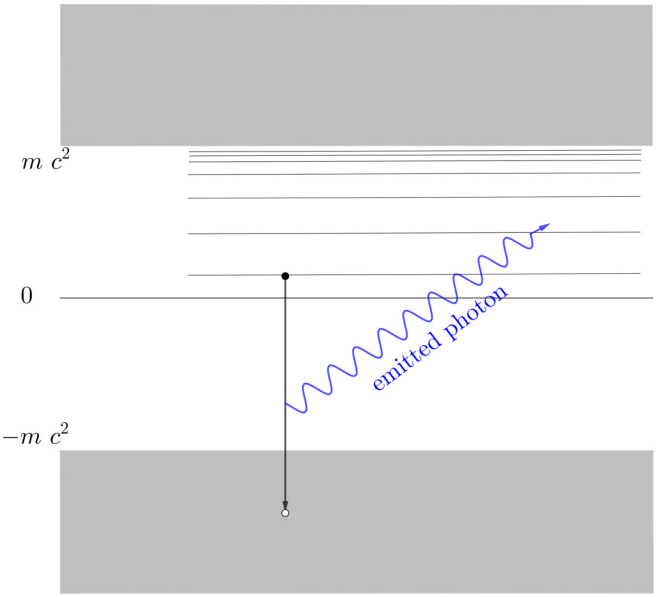

FIG. 1. A schematic illustration—within the Dirac sea picture—of annihilation of a positron on a bound electron with emission of a single photon. In this picture, the process can be viewed as a spontaneous radiative decay of a bound state into (a hole in) the negative-energy continuum.

Shimizu *et al.* [7] performed an experiment on NRA of positrons in a thin lead foil using a monoenergetic 300 keV positron beam. Taking into account the contributions to this process from the *K*-*K*, *K*-*L*, *K*-*M*, and *L*-*L* electron pairs in lead atoms, they found, for the measured cross section,

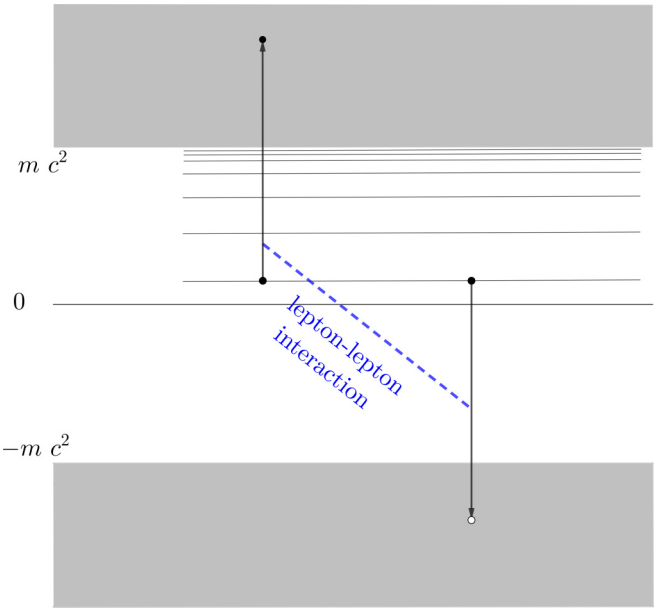

FIG. 2. A schematic illustration—within the Dirac sea picture—of nonradiative annihilation of a positron on bound electrons. This process can be viewed as a kind of autoionization in which one of the electrons undergoes a transition filling a hole in the negative-energy continuum, whereas the other is emitted carrying away the energy release.

$\sigma_{\rm exp} \sim 0.8 \times 10^{-26}$ cm^2. The authors of [7] also made calculations for NRA involving various pairs of active electrons and obtained the cross-section value of $\approx 0.73 \times 10^{-26}$ cm^2, which is quite close to their measured cross section.

Nonradiative annihilation was also considered by Mikhailov and Porsev [8,9], who used approximate wave functions to describe the electrons and the positron. In [8], the Darwin approximation and Furry-Sommerfeld-Maue wave functions were employed to describe bound electrons and the positive- and negative-energy continuum states, respectively. In [9], a term $\sim Z^2\alpha^2$ was added in the expansion of the wave functions, both for bound and continuum states. The authors derived a simple analytical expression for the total cross and obtained cross-section values which are two orders of magnitude smaller than those reported in previous works [5–7]. The results of [8,9] were slightly corrected in a recent book [10].

As it follows from the brief discussion given in the previous paragraphs, the studies of NRA produced contradicting results for the cross sections. To our knowledge, this point was not clarified in the literature. It is, therefore, the main intention of the present paper to give a detailed theoretical description of this process and present accurate numerical results for its cross sections.

The paper is organized as follows. In the next section, using the *S*-matrix formalism, we give a fully relativistic description of NRA. Section III contains results and discussion. In particular, in this section we not only present results for nonradiative annihilation, but also compare this process with radiative annihilation proceeding with emission of a single photon. In addition, we use our results for nonradiative annihilation and the principle of detailed balance to get cross sections for the process of negative-continuum dielectronic recombination, obtaining a very good agreement with the direct calculations for this process [11–13]. Section IV contains concluding remarks.

Atomic units ($m_e = \hbar = e = 1$, where m_e is the electron mass, $\hbar$ is the Planck constant, and e is the elementary charge) are used throughout, except where otherwise stated.

II. GENERAL CONSIDERATION

According to the "Dirac sea" picture, proposed by Dirac to keep atoms stable in their ground states, under the normal conditions all negative-continuum electron states are occupied. In this picture, the process of positron-electron annihilation is viewed as a transition of a positive-energy electron to a vacancy in the negative-energy continuum. The corresponding energy difference is either converted into the electromagnetic radiation (radiative annihilation) or is transferred to a matter particle represented, in our case, by a neighbor (assisting) electron (nonradiative annihilation).

Let us consider a system consisting of an incident positron and two electrons which are initially tightly bound by the field of a highly charged nucleus. The process of NRA can be conveniently described using the *S*-matrix formalism. Taking into account that in the Dirac sea picture the positron and the electron to be annihilated are viewed as two different states of the same lepton and that the interaction between this lepton and the assisting electron is transmitted by the

electromagnetic field, the transition matrix element reads (see, e.g., [14])

$$S_{fi} = -\frac{i}{c^2}\int d^4\mathsf{x}\, d^4\mathsf{y} J^{\mu}_{+}(\mathsf{x}) D_{\mu\nu}(\mathsf{x}-\mathsf{y}) J^{\nu}_{-}(\mathsf{y}). \quad (1)$$

Here, $J_+(\mathsf{x})$ is the electromagnetic four-current (density) at a space-time point x describing the transition of one of the electrons from its initial bound state into a vacancy in the negative-energy continuum, and $J_-(\mathsf{y})$ is the electromagnetic four-current at a space-time y corresponding to the transition of the other (assisting) electron from its initial bound state to the positive-energy continuum. Further, $D_{\mu\nu}(\mathsf{x}-\mathsf{y})$ is the propagator of the electromagnetic field which transmits the interaction between the two four-currents and c is the speed of light. The contravariant, $a^\mu = (a_0, \mathbf{a})$, and covariant, $a_\mu = (a_0, -\mathbf{a})$, four-vectors are related by $a_\mu = \mathrm{g}_{\mu\nu}a^\nu$, where the metric tensor $\mathrm{g}_{\mu\nu}$ is defined according to $\mathrm{g}_{00} = -\mathrm{g}_{11} = -\mathrm{g}_{22} = -\mathrm{g}_{33} = 1$ and $\mathrm{g}_{\mu\nu} = 0$ for $\mu \neq \nu$. In Eq. (1) and below, the summation over the repeated Greek indices is implied.

Below, the S-matrix transition element will be evaluated based on the following. First, it is convenient to work in a reference frame where the heavy nucleus is at rest and to take its position as the origin. Second, the field of the highly charged nucleus is much stronger than the fields produced by the leptons. Therefore, the interaction between each of the leptons and the field of the nucleus will be taken into account exactly via using the corresponding Dirac wave functions for describing both the bound and continuum states of the leptons. Third, the interaction between the electron-positron pair and the remaining electron will be taken in the lowest possible (=first) order of the perturbation theory. Fourth, since the electrons are indistinguishable, the exchange effect has to be taken into account. This will be done by antisymmetrizing the initial wave function of the two electrons.

Thus, the transition S-matrix element can be written as a sum of the direct, S^{dir}_{fi}, and exchange, S^{exc}_{fi}, terms,

$$S_{fi} = S^{\mathrm{dir}}_{fi} + S^{\mathrm{exc}}_{fi}. \quad (2)$$

The direct part reads

$$S^{\mathrm{dir}}_{fi} = -\frac{i}{c^2}\int d^4\mathsf{x}\, d^4\mathsf{y} J^{\mu}_{\mathrm{dir},+}(\mathsf{x}) D_{\mu\nu}(\mathsf{x}-\mathsf{y}) J^{\nu}_{\mathrm{dir},-}(\mathsf{y}), \quad (3)$$

where the four-currents are given by

$$J^{\mu}_{\mathrm{dir},+}(\mathsf{x}) = ec\,\overline{\psi}_{c,+}(t_1,\mathbf{x})\gamma^\mu\psi_a(t_1,\mathbf{x}) \quad (4)$$

for a transition to the positive-energy continuum and by

$$J^{\mu}_{\mathrm{dir},-}(\mathsf{y}) = ec\,\overline{\psi}_{c,-}(t_2,\mathbf{y})\gamma^\mu\psi_b(t_2,\mathbf{y}) \quad (5)$$

for a transition to the negative-energy continuum. In these expressions, ψ_a and ψ_b are single-electron bound wave functions referring to the initial states of the electrons in the field of the highly charged ion, and ψ_{c+} and ψ_{c-} are continuum wave functions describing states with the positive and negative energies, respectively. Further, $\mathsf{x} = (t_1, \mathbf{x})$ and $\mathsf{y} = (t_2, \mathbf{y})$, where $\mathbf{x}$ and $\mathbf{y}$ are the three-dimensional position vectors of the electrons with respect to the nucleus, γ^μ are the Dirac γ-matrices, and the notation $\overline{\psi}$ stands for the adjoint conjugate $\overline{\psi} = (\gamma_0\psi)^\dagger$.

Similarly, the exchange term is given by

$$S^{\mathrm{exc}}_{fi} = +\frac{i}{c^2}\int d^4\mathsf{x}\, d^4\mathsf{y} J^{\mu}_{\mathrm{exc},+}(\mathsf{x}) D_{\mu\nu}(\mathsf{x}-\mathsf{y}) J^{\nu}_{\mathrm{exc},-}(\mathsf{y}), \quad (6)$$

where

$$J^{\mu}_{\mathrm{exc},+}(\mathsf{x}) = ec\,\overline{\psi}_{c,+}(t_1,\mathbf{x})\gamma^\mu\psi_b(t_1,\mathbf{x}) \quad (7)$$

and

$$J^{\mu}_{\mathrm{exc},-}(\mathsf{y}) = ec\,\overline{\psi}_{c,-}(t_2,\mathbf{y})\gamma^\mu\psi_a(t_2,\mathbf{y}). \quad (8)$$

A. Bound-state wave functions

As stated above, ψ_a and ψ_b are bound wave functions describing the initial single-electron states. We take them as the Dirac hydrogenlike wave functions, which read

$$\psi_\nu(t,\mathbf{x}) = e^{-i\varepsilon_\nu t}\begin{pmatrix} g_\nu(x)\,\chi^{\mu_\nu}_{\kappa_\nu}(\hat{\mathbf{x}}) \\ i f_\nu(x)\,\chi^{\mu_\nu}_{-\kappa_\nu}(\hat{\mathbf{x}}) \end{pmatrix}. \quad (9)$$

Here, $x = |\mathbf{x}|$, $\hat{\mathbf{x}} = \mathbf{x}/x$, $\nu = a$ (or $\nu = b$), ε_ν is the corresponding binding energy, and κ_ν and μ_ν are the relativistic quantum number and the magnetic quantum number, respectively, in the state ψ_ν. The functions $\chi^\mu_\kappa(\hat{\mathbf{x}})$ denote the normalized spin-angular functions and will be given below. Further, g_ν (f_ν) are the large (small) component of the Dirac radial function for the electron which moves in a spherical potential $V(x)$ created by the nucleus with a charge Z (and possibly by other atomic electrons).

In the case of a Coulomb field, $V(x) = -\frac{Ze^2}{x}$, the exact energies and the radial wave functions of the bound states are known analytically and given, respectively, by (see, e.g., [15])

$$\varepsilon_\nu = mc^2\left[1 + \left(\frac{\zeta}{n'+s}\right)^2\right]^{-\frac{1}{2}} \quad (10)$$

and

$$\begin{Bmatrix} g_\nu \\ f_\nu \end{Bmatrix} = -N_\pm r^{s-1}e^{-\frac{r}{2}}\left[\left(\kappa - \frac{\zeta}{q\lambda\!\!\!^{-}_e}\right){}_1F_1(-n', 2s+1, r) \pm n'\,{}_1F_1(-n'+1, 2s+1, r)\right]. \quad (11)$$

Here, $\zeta = Z\alpha$, where $\alpha = e^2/\hbar c \simeq 1/137$ is the fine-structure constant, $s = \sqrt{\kappa^2 - \zeta^2}$, $r = 2qx$, $n' = n - |\kappa|$, and

$$N_\pm = \pm\left(1 \pm \frac{\varepsilon_\nu}{mc^2}\right)^{\frac{1}{2}} \frac{\sqrt{2}q^{\frac{5}{2}}\lambda\!\!\!^{-}_e}{\Gamma(2s+1)}\left[\frac{\Gamma(2s+n'+1)}{n'!\zeta(\zeta - \kappa q\lambda\!\!\!^{-}_e)}\right]^{\frac{1}{2}}. \quad (12)$$

In expressions (11) and (12), the signs + and − (in the notation $\pm$) refer to g_ν and f_ν, respectively. Further, $\Gamma(x)$ and ${}_1F_1(a,b;z)$ are the gamma and confluent hypergeometric functions [16], respectively, $\lambda\!\!\!^{-}_e = \hbar/mc$ is the electron Compton wavelength, and $q = \frac{\zeta}{\lambda\!\!\!^{-}_e}[\zeta^2 + (n'+s)^2]^{-\frac{1}{2}}$. The normalized spin-angular function χ^μ_κ for a fixed quantum number κ and magnetic quantum number μ (see, e.g., [15,17]) reads

$$\chi^\mu_\kappa(\hat{\mathbf{x}}) = \sum_{m_s=\pm\frac{1}{2}} C^{j\mu}_{l\mu-m_s\frac{1}{2}m_s} Y_{l\mu-m_s}(\hat{\mathbf{x}})\ \chi^{m_s}_{\frac{1}{2}}, \quad (13)$$

where $C^{j\mu}_{lm\,\frac{1}{2}m_s}$ and Y_{lm} are the Clebsch-Gordon coefficients and the spherical harmonic functions [18], respectively, l and j are the orbital and total angular momenta, $l=\kappa$ if $\kappa>0$; $l=-\kappa-1$ if $\kappa<0$ and $j=|\kappa|-\frac{1}{2}$, and the quantities $\chi^{m_s}_{\frac{1}{2}}$ are the Pauli spinors with $\chi^{\frac{1}{2}}_{\frac{1}{2}}=\binom{1}{0}$ and $\chi^{-\frac{1}{2}}_{\frac{1}{2}}=\binom{0}{1}$.

B. Continuum wave functions

1. Positive-energy continuum

The electron emitted in the process of NRA is represented by a positive-energy continuum state. For an electron with the total energy $E_k>mc^2$, which moves in a spherical potential field, its state can be written in the form

$$\psi_{c+}(t_1,\mathbf{x})=\ e^{-iE_k\,t_1}\ \psi^{(-)m_s}_{\mathbf{k}}(\mathbf{x}), \tag{14}$$

where $\psi^{(-)m_s}_{\mathbf{k}}(\mathbf{x})$ is the incoming wave with an asymptotic momentum $\mathbf{k}$ and a spin projection m_s. Choosing the z axis to be the quantization axis, the wave function $\psi^{(-)m_s}_{\mathbf{k}}(\mathbf{x})$ can be written as (see, e.g., [15,17])

$$\psi^{(-)m_s}_{\mathbf{k}}(\mathbf{x})=4\pi\sqrt{\frac{\pi}{V_e 2W_k k}}\sum_{\kappa\mu} i^l e^{-i\Delta_\kappa} C^{j\mu}_{lm\,\frac{1}{2}m_s} Y^*_{l\mu-m_s}(\hat{\mathbf{k}})\varphi_{E_k\kappa\mu}(\mathbf{x}), \tag{15}$$

where V_e is the normalization volume for the emitted electron with an energy $E_k=W_k mc^2$, and

$$\varphi_{E_k\kappa\mu}(\mathbf{x})=\begin{pmatrix} P_\kappa(x)\ \chi^\mu_\kappa(\hat{\mathbf{x}}) \\ iQ_\kappa(x)\ \chi^\mu_{-\kappa}(\hat{\mathbf{x}})\end{pmatrix}. \tag{16}$$

The functions P_κ and Q_κ are the radial solutions of the system of coupled Dirac equations in a spherical potential $V(x)$. In the case of a Coulomb potential, produced by a pointlike nucleus of charge Z, the exact radial solutions read (see, e.g., [15,17])

$$\begin{Bmatrix} P_\kappa \\ Q_\kappa\end{Bmatrix}=A_\pm\varrho^{s-1}\begin{Bmatrix}\mathrm{Re}\\ \mathrm{Im}\end{Bmatrix} e^{-\frac{i}{2}\varrho}e^{i\delta_\kappa}(s+i\eta)\ {}_1F_1(i\eta+s+1,2s+1,i\varrho). \tag{17}$$

Here, $\varrho=2kx$,

$$A_\pm=\pm(E_k\pm mc^2)^{\frac{1}{2}}\frac{2k^{\frac{1}{2}}}{c\sqrt{\pi}}\frac{|\Gamma(s+i\eta)|}{\Gamma(2s+1)}e^{\frac{\pi}{2}\eta}, \tag{18}$$

where $+$ and $-$ refer to P_κ and Q_κ, respectively, the notation Re (Im) denotes the real (imaginary) part of the term on the right-hand side of (17), $\eta=Z\alpha\frac{E_k}{ck}$ is the Sommerfeld parameter, and the phase δ_κ is defined by

$$e^{2i\delta_\kappa}=\frac{-\kappa+i\eta/W_k}{s+i\eta}. \tag{19}$$

The Coulomb phase shift Δ_κ is given by $\Delta_\kappa=\delta_\kappa-\arg\Gamma(s+i\eta)+(l+1-s)\frac{\pi}{2}$ (see, e.g., [15]).

2. Negative-energy continuum

The incoming negative-energy ($-E_p<0$) continuum state of an electron moving along the z axis (taken as the quantization axis) with an asymptotic momentum $\mathbf{p}$ and helicity σ can be written as

$$\psi_{c-}(t,\mathbf{x})=\ e^{+iE_p\,t}\psi^{(-)}_{\mathbf{p},\sigma}(\mathbf{x}), \tag{20}$$

where, taking into account that $\sigma=-2m'_s$, one has

$$\psi^{(-)}_{\mathbf{p},m'_s}(\mathbf{x})=\sqrt{\frac{4\pi^2}{V_p\,2W_p\,p}}\sum_{\kappa'} i^{l'}e^{-i\Delta'_{\kappa'}}\sqrt{2l'+1}\ C^{j'm'_s}_{l'0\,\frac{1}{2}m'_s}\psi_{E_p\kappa'm'_s}(\mathbf{x}), \tag{21}$$

where V_p is the normalization volume for the positron with an energy $E_p=W_pmc^2$. The partial wave function $\psi_{E_p\kappa m_s}$, which describes a negative-energy electron with a given quantum number κ and a projection m_s of the spin along the z axis moving in the field of a spherically symmetric potential, can be taken in the form

$$\phi_{E_p\kappa m_s}(\mathbf{x})=\begin{pmatrix} -iF_\kappa(x)\ \chi^{m_s}_{-\kappa}(\hat{\mathbf{x}}) \\ G_\kappa(x)\ \chi^{m_s}_{\kappa}(\hat{\mathbf{x}})\end{pmatrix}, \tag{22}$$

where

$$\begin{Bmatrix} G_\kappa \\ F_\kappa\end{Bmatrix}=B_\pm\varrho^{s-1}\begin{Bmatrix}\mathrm{Re}\\ \mathrm{Im}\end{Bmatrix} e^{-\frac{i}{2}\varrho}e^{i\delta'_\kappa}(s+i\eta')\ {}_1F_1(i\eta'+s+1,2s+1,i\varrho), \tag{23}$$

with $\varrho=2p\,x$ and

$$B_\pm=\pm(E_p\pm mc^2)^{\frac{1}{2}}\frac{2p^{\frac{1}{2}}}{c\sqrt{\pi}}\frac{|\Gamma(s+i\eta')|}{\Gamma(2s+1)}e^{-\frac{\pi}{2}\eta'}. \tag{24}$$

Here, $\eta'=-Z\alpha\frac{E_p}{c\,p}$ and $\delta'_\kappa=\frac{1}{2}\arg[-s\kappa W_p+\eta'^2+i\eta'(\kappa W_p+s)]+\xi\frac{\pi}{2}$, with $\xi=1$ if $\kappa>0$ and $\xi=0$ if $\kappa<0$. The Coulomb phase shift $\Delta'_\kappa=\delta'_\kappa-\arg\Gamma(s+i\eta')+(l+1-s)\frac{\pi}{2}$, where $l=\kappa$ if $\kappa>0$ and $l=-\kappa-1$ if $\kappa<0$. Further, $s=\sqrt{\kappa^2-\zeta^2}$ as before and $W_p=\frac{E_p}{mc^2}>0$ is the Lorentz factor of the positron.

C. Cross sections

The cross section is related to the S-matrix transition element by the standard rules. In particular, the cross section for NRA, which is the differential in the energy and angle of the emitted electron, reads

$$\frac{d\sigma^{\mathrm{NRA}}}{dE_k d\Omega_k}=\frac{\pi^2c^2\alpha^2}{v_p\,pW_p}\left[\frac{1}{2}\sum_{m'_s m_s}\right]\sum_{\mu_a\mu_b}|T_{fi}|^2\delta(\varepsilon_a+\varepsilon_b+E_p-E_k). \tag{25}$$

Here, v_p is the (asymptotic) velocity of the incident positron, p and $E_p=mc^2W_p$ are its momentum and energy, respectively, ε_a and ε_b are the binding energies of the electrons in their initial states, E_k is the energy of the emitted electron, and Ω_k is its emission (solid) angle. In Eq. (25), the averaging over the positron spin and summation over the spin of the emitted electron are performed. Further,

$$T_{fi}=\sum_{\kappa\mu\kappa'} i^{l'-l}C^{j\mu}_{l\mu-m_s;\frac{1}{2}m_s}C^{j'\mu'}_{l'0;\frac{1}{2}m'_s}Y_{l\mu-m_s}(\hat{\mathbf{k}})e^{i(\Delta_\kappa+\Delta'_{\kappa'})}\mathcal{M}_{fi}, \tag{26}$$

TABLE I. The total cross section for NRA of a positron with kinetic energy of 500 keV on the K shell of gold ($Z = 79$) and lead ($Z = 82$).

$\sigma^{\rm NRA}$ (10^{-27} cm^2)		
$Z = 79$	$Z = 82$	
	2	Ref. [6]
	1.5	Ref. [7]
1.3×10^{-2} [a]	1.5×10^{-2} [a]	Ref. [10]
0.4×10^{-1}	0.52×10^{-1}	Present work

[a]Expression (11.68) from [10].

where $\mathcal{M}_{fi} = \frac{1}{\sqrt{2}}(\mathcal{M}^{\rm dir}_{fi} - \mathcal{M}^{\rm exc}_{fi})$. The direct term $\mathcal{M}^{\rm dir}_{fi}$ reads

$$\mathcal{M}^{\rm dir}_{fi} = \frac{1}{2\pi^2}\int d^3\boldsymbol{\kappa}\frac{g_{\alpha\beta}}{\boldsymbol{\kappa}^2 - \left(\frac{\omega_{fi}}{c}\right)^2 - i0^+}\int d^3\mathbf{x}\ e^{-i\mathbf{x}\cdot\boldsymbol{\kappa}}\overline{\varphi}_{E_k\kappa\mu}(\mathbf{x}) \times\gamma^\alpha\varphi_a(\mathbf{x})\int d^3\mathbf{y}\ e^{i\mathbf{y}\cdot\boldsymbol{\kappa}}\ \overline{\psi}_{E_p\kappa' m'_s}(\mathbf{y})\gamma^\beta\varphi_b(\mathbf{y}). \quad (27)$$

The exchange term $\mathcal{M}^{\rm exc}_{fi}$ is obtained from the direct one by interchanging the states φ_a and φ_b.

The total cross section is obtained by integrating (25) over the energy and angles of the emitted electron. The integration over the energy is performed with the help of the δ function. The integration over the solid angle and the summation over the electron spin m_s are performed by using the properties of the spherical harmonics and the Clebsch-Gordon coefficients, respectively. The result is

$$\sigma^{\rm NRA} = \frac{\pi^2 c^2\alpha^2}{v_p\, pW_p}\left[\frac{1}{2}\sum_{m'_s}\right]\sum_{\mu_a\mu_b}\sum_{\kappa'\kappa\mu}|\mathcal{M}_{fi}|^2. \quad (28)$$

III. RESULTS AND DISCUSSION

In this section, we consider numerical results for nonradiative annihilation, which are obtained by using the treatment of this process discussed in the previous section. We shall compare them (when possible) with results for this process obtained by other authors. We shall also use our results for NRA to get the total cross section for its inverse process. Besides, we shall compare the cross sections for NRA and radiative annihilation with emission of a single photon.

A. Nonradiative annihilation of a positron on the K-shell electrons

In Table I, we present results for the total cross section for NRA of a 500 keV positron on the K-shell electrons in Au ($Z = 79$) and Pb ($Z = 82$). It follows from the table that our results agree neither with those of [6,7] nor with those obtained using expression (11.68) of [10]. In particular, our results are much smaller than those of [6,7], but exceed, roughly by a factor of 3, the results of [10].

Moreover, it turns out that the different calculations predict even a different shape for the total cross section considered as a function of the energy of the incident positron. This is clearly seen in Fig. 3, where we present the total cross section for NRA of positrons on the K-shell electrons in lead [Pb ($Z = 82$)] given as a function of the positron kinetic energy. Indeed, while at small positron energies all the calculations show an increase in the cross section with the growth in the impact energy, they predict different positions of its maximum. In addition, at larger impact energies, where the cross section decreases, they predict, for this decrease, different rates. In particular, at large positron energies, our results show a much more extended cross-section tail compared to the other calculations.

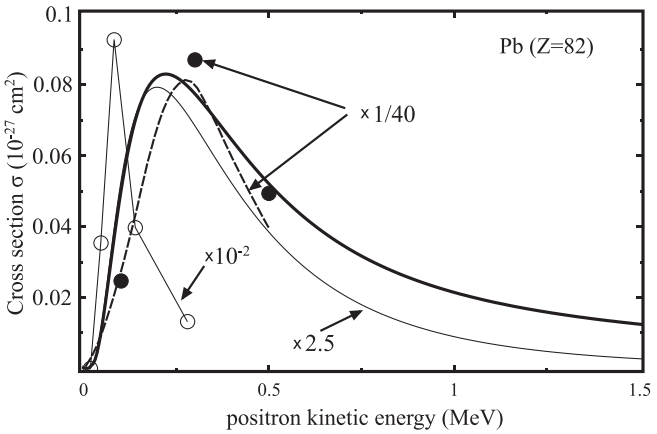

FIG. 3. Cross sections for NRA of the incident positron on the K shell of lead. Solid circles: results of [6] divided by 40; open circles connected by a thin line: results from [5] divided by 100; dashed line: results of [7] divided by 40; thin solid line: results obtained by using Eq. (11.68) of [10] multiplied by 2.5; thick solid line: results of the present paper.

From the results of other authors, which are shown in Fig. 3, the closest to ours are those of [10]. If one would disregard the (substantial) difference in the absolute cross-section values, then at relatively low impact energies, our results in Fig. 3 would be rather close to those of [10]. However, at larger impact energies (after the corresponding cross-section maxima), the difference between these results rapidly grows and, at 1.5 MeV, already exceeds a factor of 7.

With increasing Z, the full account of the relativistic effects becomes more and more important. Therefore, as one can expect, the difference between our results and those of [10] grows when Z increases. For instance, comparing the results for NRA on the K shell of plutonium (see Fig. 4) with those for lead (see Fig. 3), we see that this difference noticeably increases both at the maximum of the calculated cross sections and at larger impact energies, reaching a factor of 10 at an energy of 1.5 MeV.

Figure 5 shows the total cross section for NRA of a positron on the K shell of different elements ranging from $Z = 47$ to $Z = 100$. The cross section is given as a function of the kinetic energy of the incident positron. It, in particular, follows from this figure that the cross section rapidly grows when the atomic number Z increases. For instance, the ratio between the maximum values of the cross section at $Z = 47$ and $Z = 100$ reaches almost a factor of 150, suggesting the corresponding cross-section dependence $\sim Z^\rho$ with $\rho \approx 6.7$.

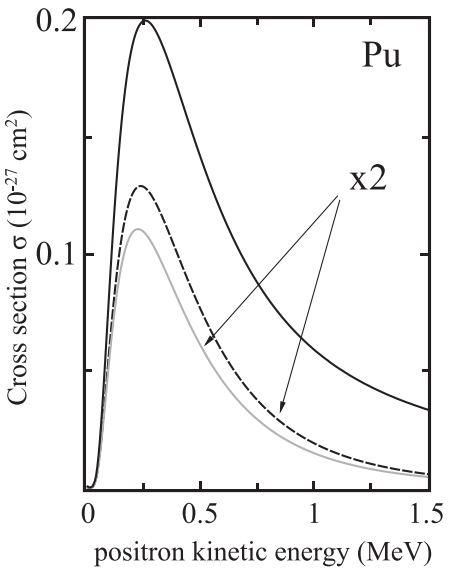

FIG. 4. The total cross section for NRA of a positron on the K shell of plutonium ($Z = 94$). Dashed and thin-solid gray lines are twice the results obtained by using Eqs. (11.64) and (11.68), respectively, from [10]. Thick-solid line is the results of the present paper.

B. Nonradiative annihilation of a positron involving electron(s) from the L and M shells

In the previous sections, we considered NRA on the K-shell electrons only. Now we very briefly discuss NRA involving (also) electrons from higher shells. In Table II, we present the total cross sections for NRA of a positron by various combinations of electron pairs in gold and lead. The cross sections are given at those positron energies where they reach their maximal values; the corresponding positron energies are also indicated.

TABLE II. Cross sections (in 10^{-27} cm^2) for NRA of a positron on various pairs of electrons in gold ($Z = 79$, left column) and lead ($Z = 82$, right column). The cross sections are given at those positron energies where they reach their maximum; the corresponding kinetic energies of the positron are indicated.

	The cross sections for NRA (in 10^{-27} cm^2)			
	$Z = 79$ at $E_p = 231.6$ keV		$Z = 82$ at $E_p = 220.9$ keV	
K-K	0.652×10^{-1}		0.831×10^{-1}	
K-L_I		0.191×10^{-1}		0.247×10^{-1}
K-L_{II}		0.36×10^{-2}		0.501×10^{-2}
K-L_{III}		0.18×10^{-2}		0.246×10^{-2}
K-L	0.245×10^{-1}		0.321×10^{-1}	
K-M_I		0.558×10^{-2}		0.719×10^{-2}
K-M_{II}		0.122×10^{-2}		0.170×10^{-2}
K-M_{III}		0.66×10^{-3}		0.890×10^{-3}
K-M_{IV}		0.72×10^{-5}		0.105×10^{-4}
K-M_V		0.15×10^{-4}		0.222×10^{-4}
K-M	0.75×10^{-2}		0.98×10^{-2}	
L_I-L_I		0.14×10^{-2}		0.18×10^{-2}
L_I-L_{II}		0.48×10^{-3}		0.68×10^{-3}
L_I-L_{III}		0.26×10^{-3}		0.36×10^{-3}
L_{II}-L_{II}		0.45×10^{-5}		0.72×10^{-5}
L_{II}-L_{III}		0.66×10^{-4}		0.984×10^{-4}
L_{III}-L_{III}		0.59×10^{-5}		0.833×10^{-5}
L-L	$\simeq 0.22 \times 10^{-2}$		$\simeq 0.30 \times 10^{-2}$	
σ_{total}	$\simeq 0.1$		$\simeq 0.125$	

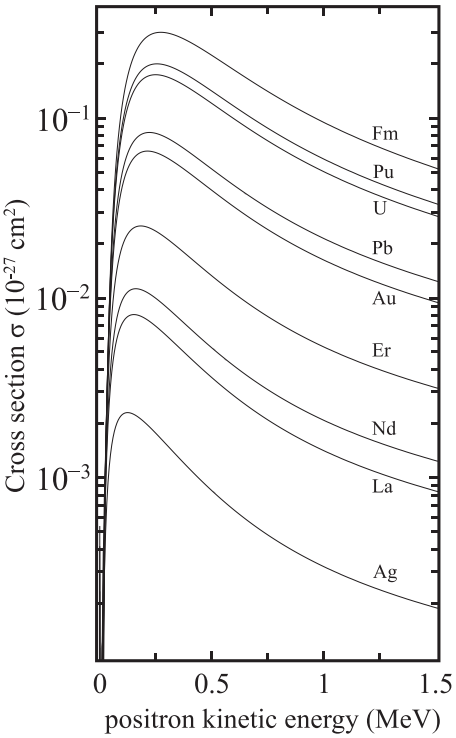

FIG. 5. The total cross section for NRA of a positron on the K shell of elements with the atomic numbers ranging between $Z = 47$ and $Z = 100$ given as a function of the positron kinetic energy.

The cross sections were calculated assuming that the active electrons move in the unscreened field of the nucleus. This is a rather rough approximation since in real systems this field will be partly screened by other atomic (or ionic) electrons. The screening has the smallest effect on the K shell and its relative importance rapidly grows with the increase in the shell number. The neglect of the screening reduces the size of the electron orbits, decreasing the distance between the active electrons. This effectively increases the strength of the lepton-lepton interaction and, as a result, the probability for nonradiative annihilation.

Thus, our results for nonradiative annihilation, which involves active electrons from the L and M shells, would noticeably overestimate the corresponding cross sections for many-electron ions and neutral atoms. However, as it follows from Table II, even overestimated values for annihilation involving the K-L, K-M, and L-L electron pairs remain substantially smaller than the K-K annihilation cross section. This enables us to conclude that even in neutral heavy atoms, nonradiative annihilation will mainly proceed on the K shell and that the corresponding results (which were obtained essentially

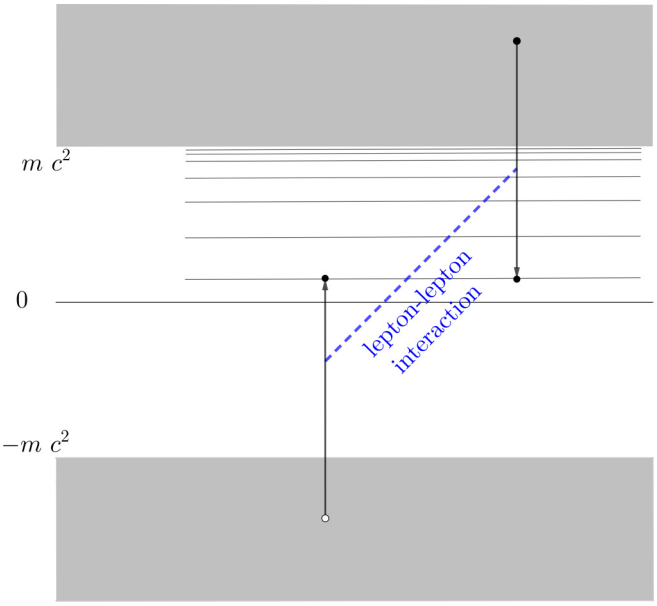

FIG. 6. A scheme of the process of negative-continuum dielectronic recombination (NCDR).

for heliumlike ions) could also serve—as an estimate—for annihilation on neutral atoms.

C. Nonradiative annihilation and negative-continuum dielectronic recombination

Taking into account large differences between our results and those of the other authors, we made an additional check of our calculations by considering the process of so-called negative-continuum dielectronic recombination (NCDR) [11–13]. In the process of NCDR, an electron incident on a bare nucleus is captured, forming a bound state with the nucleus. The energy that is released in the capture is converted into an electron-positron pair, with the electron being created in a bound state. In the Dirac sea picture, this process can be viewed as dielectronic recombination involving a negative-energy electron (see Fig. 6), which plays the same role as a bound "real" electron in the usual dielectronic recombination. As a result of the interaction between the incident and a negative-energy electron, both undergo transitions into bound states, leaving a hole in the negative-energy continuum which corresponds to an emitted positron.

As is obvious from the above brief description, the process of NCDR is inverse to the process of NRA. This means that the cross section for NCDR can be calculated by using the cross section for NRA and employing the principle of detailed balance.

Table III presents a comparison between results for NCDR, which were obtained in Ref. [11] and in the present paper. According to the remark made in Ref. [13], the cross-section values of [11] were corrected by multiplying them by the factor W_p/p. Our results were calculated by using Eqs. (28) and the principle of detailed balance. It follows from the tables that the agreement is quite good, which lends further support to the accuracy of the results for NRA presented in this paper.

D. Nonradiative annihilation vs single-photon radiative annihilation

Let us now briefly discuss the correspondence between nonradiative and single-photon radiative annihilation processes. Our results for the total cross section for single-photon

TABLE III. The total cross section for the NCDR reaction $e^- + U^{92+} \rightarrow U^{90+}(1s^2) + e^+$ obtained in Ref. [11] and in the present paper. We note that the results of [11] were multiplied by the factor W_p/p (see [13]). The total cross section for the inverse reaction (NRA), $e^+ + U^{90+}(1s^2) \rightarrow U^{92+} + e^-$, is also given. For more explanation, see the text.

Kinetic energies (keV)		Cross sections (10^{-27} cm^2)		
Positron	Electron	NRA	NCDR[a]	NCDR[b]
42.56	800	8.2×10^{-3}	2.55×10^{-4}	2.44×10^{-4}
92.56	850	7.18×10^{-2}	4.65×10^{-3}	4.53×10^{-3}
142.6	900	1.33×10^{-1}	1.27×10^{-2}	1.243×10^{-2}
192.6	950	1.64×10^{-1}	2.05×10^{-2}	2.08×10^{-2}
242.6	1000	1.74×10^{-1}	2.64×10^{-2}	2.59×10^{-2}
342.6	1100	1.61×10^{-1}	3.22×10^{-2}	3.16×10^{-2}
442.6	1200	1.35×10^{-1}	3.29×10^{-2}	3.22×10^{-2}
542.6	1300	1.11×10^{-1}	3.12×10^{-2}	3.05×10^{-2}
642.6	1400	9.12×10^{-2}	2.88×10^{-2}	2.81×10^{-2}
742.6	1500	7.58×10^{-2}	2.63×10^{-2}	2.56×10^{-2}
842.6	1600	6.40×10^{-2}	2.39×10^{-2}	2.33×10^{-2}
942.6	1700	5.48×10^{-2}	2.19×10^{-2}	2.14×10^{-2}
1043	1800	4.76×10^{-2}	2.02×10^{-2}	1.96×10^{-2}
1143	1900	4.19×10^{-2}	1.87×10^{-2}	1.81×10^{-2}
1243	2000	3.72×10^{-2}	1.73×10^{-2}	1.68×10^{-2}
1743	2500	2.33×10^{-2}	1.27×10^{-2}	1.23×10^{-2}
2243	3000	1.62×10^{-2}	9.83×10^{-3}	9.5×10^{-3}

[a]Results for NCDR obtained by using Eq. (28) and the principle of detailed balance.
[b]Results of [11] multiplied by the factor W_p/p.

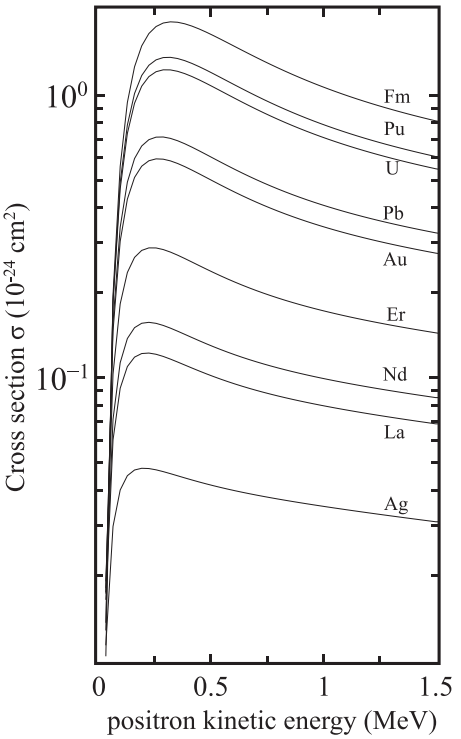

FIG. 7. The total cross section for single-photon annihilation of a positron on the K shell of elements with the atomic numbers ranging between $Z = 47$ and $Z = 100$ given as a function of the positron kinetic energy.

annihilation of a positron on the K shell are shown in Fig. 7. By comparing them with the corresponding results for NRA (see Fig. 5), one can make a few main observations. First, annihilation with emission of a photon is much more probable than that with emission of an electron. Second, compared to NRA, the cross section for the radiative annihilation, after reaching the maximum, decreases much slower with increasing the positron energy. Third, the ratio between the nonradiative and radiative cross section increases when Z grows.

As was already mentioned, annihilation with emission of a single photon can be regarded as spontaneous radiative decay of a bound state into the negative-energy continuum (see Fig. 1), while NRA can be viewed as autoionization (involving transitions to the negative-energy continuum; see Fig. 2). Therefore, it is of interest to make a brief comparison of the correspondence between these processes with that between the "normal" spontaneous radiative decay and autoionization of excited electron states.

It is known that in highly charged ions, where the latter processes are characterized by a large energy release, the process of spontaneous radiative decay is much stronger than autoionization (Auger decay). Besides, when the atomic number of the ion grows—which also leads to the increase in the energy release—the dominance of the radiative decay over autoionization increases.

In annihilation, where the energy release is very large, the "spontaneous radiative decay" also strongly dominates over "autoionization." In addition, in annihilation the energy release depends mainly on the positron energy (and just rather weakly on Z) and we observe that the dominance of the "spontaneous radiative decay" grows with increasing this energy. We thus see that the correspondence between "radiative decay" and "autoionization" channels of annihilation is rather similar to that between the spontaneous radiative and Auger decay of excited electron states in highly charged ions.

On the other hand, since the energy release in annihilation weakly depends on Z whereas the effective strength of the electron-electron interaction increases with Z, the ratio between autoionization and spontaneous radiative decay is now different: unlike the decay of "normal" excited electron states, where the ratio decreases with Z, in the case of annihilation it grows.

IV. CONCLUSIONS

We have considered nonradiative annihilation of a positron by bound electrons in various heavy elements ranging from silver ($Z = 47$) to fermium ($Z = 100$). Our consideration was based on the fully relativistic treatment of this process which employs the exact (Dirac) positive- and negative-energy continuum states as well as bound states to describe the motion of the leptons in a strong Coulomb field of the nucleus. The interaction between the leptons, which is much weaker than their interaction with the nucleus, was taken into account in the lowest possible order of perturbation theory.

The main focus of the present study was on nonradiative annihilation of a positron on the ground state of heliumlike heavy ions. These results can also be directly applied to estimate nonradiative annihilation on the K shell of the corresponding heavy ions with more electrons and neutral atoms.

Using the principle of detailed balance, we applied our results for nonradiative annihilation to calculate the cross section for negative-continuum dielectronic recombination. A good agreement with the existing data was found.

Our results for nonradiative annihilation involving the K-shell electrons turned out to very substantially differ from those reported by other authors. However, since (unlike the other authors) we employed the fully relativistic description of this process and used exact (Dirac) states to account for the strong interaction between the leptons and the highly charged nucleus, we expect that at the moment our results represent the most accurate data for the total cross section of this process.

We also very briefly discussed nonradiative annihilation which involves electron(s) from higher shells. According to our results, annihilation in such a case is less probable and, even in the case of a neutral atom, the main contribution to the total nonradiative annihilation of a positron will be given by the K-shell electrons.

We also compared nonradiative and single-photon radiative annihilation and found that nonradiative annihilation is a much weaker process. We discussed the correspondence between these two processes and pointed out certain similarities and differences between this correspondence and the relationship between spontaneous radiative and Auger decay of excited electron states in highly charged ions.

ACKNOWLEDGMENTS

We acknowledge the support from the National Key Research and Development Program of China (Grant No.

2017YFA0402300), the CAS President's International Fellowship Initiative, and the German Research Foundation (DFG) under Grant No. 349581371 (Project No. VO 1278/4-1). A.B.V. is grateful for the hospitality of the Institute of Modern Physics.

[1] P. A. M. Dirac, Proc. Cambridge Philos. Soc. **26**, 361 (1930).
[2] E. Fermi and G. Uhlenbeck, Phys. Rev. **44**, 510 (1933).
[3] H. J. Bhabha and H. R. Hulme, Proc. R. Soc. A **146**, 723 (1934).
[4] W. R. Johnson, D. J. Buss, and C. O. Carroll, Phys. Rev. **135**, A1232 (1964).
[5] J. Brunings, Physica **1**, 996 (1934).
[6] H. S. W. Massey and E. H. S. Burhop, Proc. R. Soc. A **167**, 53 (1938).
[7] S. Shimizu, T. Mukoyama, and Y. Nakayama, Phys. Rev. **173**, 405 (1968).
[8] A. I. Mikhaîlov and S. G. Porsev, J. Phys. B **25**, 1097 (1992).
[9] A. I. Mikhaîlov and S. G. Porsev, J. Expt. Theo. Phys. **78**, 441 (1994).
[10] E. G. Drukarev and A. I. Mikhaîlov, *High-Energy Atomic Physics*, Springer Series on Atomic, Optical, and Plasma Physics Vol. 93 (Springer, Switzerland, 2016).
[11] A. N. Artemyev, T. Beier, J. Eichler, A. E. Klasnikov, C. Kozhuharov, V. M. Shabaev, T. Stöhlker, and V. A. Yerokhin, Phys. Rev. A **67**, 052711 (2003).
[12] A. N. Artemyev, V. M. Shabaev, T. Stöhlker, and A. S. Surzhykov, Phys. Rev. A **79**, 032713 (2009).
[13] V. A. Yerokhin, A. N. Artemyev, V. M. Shabaev, Th. Stöhlker, A. Surzhykov, and S. Fritzsche, Phys. Rev. A **92**, 042708 (2015).
[14] J. D. Bjorken and S. D. Drell, *Relativistic Quantum Mechanics* (McGraw-Hill, New York, 1964).
[15] M. E. Rose, *Relativistic Electron Theory* (Wiley, New York, 1961).
[16] M. Abramovitz and I. Stegun, *Handbook of Mathematical Functions* (Dover, New York, 1964).
[17] J. Eichler and W. E. Meyerhof, *Relativistic Atomic Collisions* (Academic Press, San Diego, 1995).
[18] D. A. Varshalovitch, A. N. Moskalev, and V. K. Khersonskii, *Quantum Theory of Angular Momentum* (World Scientific, Singapore, 1988).